Beat-frequency-resolved two-dimensional electronic spectroscopy with sub-10 fs visible laser pulses

TSUBOUCHI Masaaki

Ultrafast Dynamics Group, Department of Advanced Photon Research

Quantum coherence in photosynthetic proteins in solutions has recently been reported and is actively discussed.[1] A pair of photoexcited adjacent chromophores can form exciton states. When the chromophores are excited by an ultrashort laser pulse with a spectrum broad enough to cover the split energy levels of the exciton states, quantum coherence is expected to be generated in the pair of exciton states. The quantum coherence in photosynthetic proteins has been suggested to be related to the unidirectional energy flow with extremely high efficiency, which occurs during photosynthesis.[2] However, quantum coherence during photosynthesis has not yet been confirmed.

Two-dimensional electronic spectroscopy (2D-ES) has been used to analyze this problem. 2D-ES can spectrally resolve quantum states that cannot be resolved using conventional spectroscopic techniques, owing to the inhomogeneous broadening that occurs in solution; it can also map the correlation between states.[1,3] Measurement of the correlation map, as a function of the pump-probe delay, reveals a reaction pathway from a specific state excited by an initial pump pulse. However, in the time-dependent 2D electronic spectra, the quantum beat signal between the superposition states can hardly be seen because it is usually hidden by the strong stationary signal, which is not related to the temporal evolution of the coherently excited superposition states, but rather to that of the single quantum state. To overcome this difficulty in 2D-ES, beat-frequency–resolved analysis of 2D electronic spectra has been proposed to illustrate the vibronic and exciton states and the coherences between them as coherence amplitude maps.[4,5] In this study, we demonstrate the visualization of the vibrational coherences in an artificial protein, through beat-frequency–resolved 2D-ES.[6] We successfully extract the vibrational coherences behind the strong stationary signal that dominates the typical 2D spectra and the inhomogeneous broadening in the absorption spectra.

We generate sub-10 fs visible pulses using a Yb:KGW laser (1030 nm, 1.0 mJ, 10 kHz, 190 fs), followed by two pulse-compression stages. The first pulse-compression stage employs a multiplate pulse compression (MPC) technique.[7] The output from the Yb:KGW laser is loosely focused into a gas cell filled with 1.0 bar of He, to avoid nonlinear effects around the focus. The fused-silica exit window of the gas cell and the subsequent second and third fused-silica plates act as thin plates to achieve spectral broadening in our MPC setup. The output pulses are temporally compressed by two Gires–Tournois interferometer mirrors, down to 40–50 fs. The second pulse-compression stage employs spectral broadening based on laser filamentation.[8] The output pulses from the first MPC stage are focused by a concave mirror into a mixed gas cell (0.5 bar of Xe and 0.5 bar of He), generating white light via laser-based filamentation. The visible spectral part of the white light is selected using a short-pass filter. The transmitted visible pulses are recollimated and compressed using two chirp-mirror pairs. The white-light spectrum and temporal profile after pulse compression are depicted in Fig. 1(a) and (b), respectively. The pulse energy after pulse compression is approximately 4.7 μJ. The long-term power fluctuation is measured to be 0.26% (standard deviation) for 25 h.

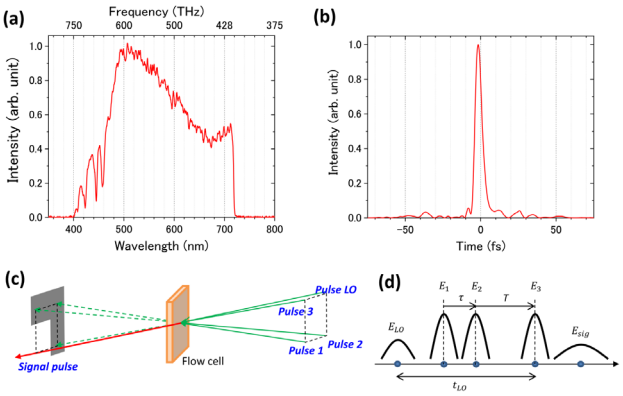

Fig. 1. (a) Spectrum and (b) temporal profile of the sub-10 fs visible pulse output after chirp-mirror-pair–based pulse compression. (c) BOXCARS geometry of four-wave mixing. (d) Time ordering of the four input pulses and signal light. E_1 and E_2 are the pump double pulses with a time interval of τ. E_3 is the probe pulse delayed from E_2 by time T. The local oscillator pulse E_{LO} is prior to the pump and probe pulses with a fixed time interval of t_{LO} between E_{LO} and E_3.

The 2D-ES measurement system is an extension of the application of 2D infrared spectroscopy[9] to the visible spectral region, to investigate the electronic states of the molecules. In 2D-ES measurement, three identical pulses (1, 2, and 3) and one weak local oscillator (LO) are focused on a sample in the BOXCARS geometry, as shown in Fig. 1(c). The signal light from the four-wave-mixing (FWM) process is spatially separated from pulses 1, 2, and 3, and interferes with the LO pulse to achieve heterodyne detection. The time ordering of the pulses and time interval between them are presented in Fig. 1(d). One of the pulses passes through the computer-controlled translational stage to scan the temporal delay, T, between pulses 2 and 3. The temporal delay, τ, between pulses 1 and 2 is scanned (or varied) by a pair of dispersion wedge plates in the optical path of pulse 1 to achieve sub-fs temporal resolution. The signal and LO pulses are spatially dispersed via holographic grating and focused on a line-scan CMOS camera.

The molecules are excited by double pulses 1 and 2 with the time interval τ, and probed by pulse 3 delayed by time T after pulse 2. The beating signal produced by the coherent excitation of a pair of vibronic states is measured by scanning the waiting time, T. Double pump pulses are used to obtain the excitation spectra. We measure the time-domain interferogram by scanning the time interval, τ, and obtain the spectrum from the Fourier transformation of the interferogram.

We apply our 2D-ES apparatus to the measurement of the vibrational coherence in a RasM monomer artificially synthesized by the Adachi Group at iQLS. The absorption spectrum of this molecule is shown in Fig. 2(a). Figure 2(b) shows the 2D power spectrum of the rephasing signal measured at a waiting time T of 40 fs. The FWM signal mainly appears in the upper-left region above the diagonal line, which means that the detection energy E_{det} is higher than the excitation energy E_{exc}. The dashed lines indicate the frequencies of the peak (E_{exc} = 512 THz) and shoulder (E_{exc} = 550 THz) in the RasM absorption spectrum.

Figure 2(c) shows the time profiles of the signal intensities at the diagonal points of (E_{exc}, E_{det}) = (512 THz, 512 THz) and (550 THz, 550 THz) and at the off-diagonal point of (E_{exc}, E_{det}) = (510 THz, 580 THz) in the 2D electronic spectra, as functions of the waiting time, T. At the diagonal points, fast oscillations that survive until T = 600 fs are clearly observed. On the other hand, at the off-diagonal point, no significant fast oscillation is observed. Figure 2(d) shows the Fourier-transformed spectra of the time profiles. The beat frequencies can be identified as E_{beat} = 35.2 THz for the time profile measured at (E_{exc}, E_{det}) = (512 THz, 512 THz), E_{beat} = 46.0 THz at (550 THz, 550 THz), and E_{beat} = 16.5 THz at (510 THz, 580 THz). These beat signals provide clear evidence of the vibrational coherence.

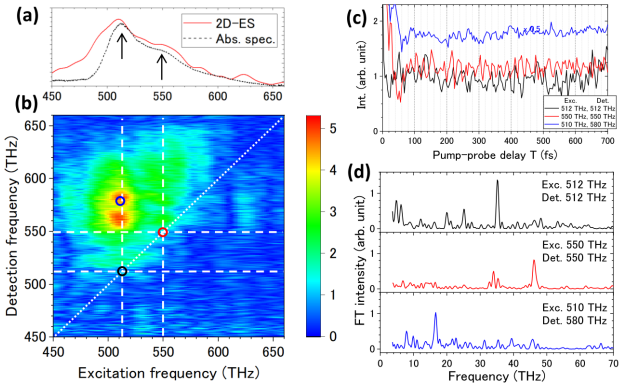

Fig. 2. (a) Absorption spectrum of the RasM monomer. (b) 2D power spectrum of the rephasing signal measured at the waiting time T of 40 fs. The white dashed lines indicate the frequencies of the peak (512 THz) and shoulder (550 THz) in the absorption spectrum of RasM. (c) Pump-probe time profiles observed at the three points of the 2D spectra shown in (a). (d) Beat-frequency spectra calculated by the Fourier transformation of the time profile shown in (c).

To further investigate the vibrational coherence, the FFT spectra of the pump-probe profiles are calculated at all excitation and detection frequencies on the 2D spectra at intervals of 4 THz. The intensity at a specific beat frequency is mapped as a function of the excitation and detection frequencies. Figure 3 shows the 2D intensity maps at E_{beat} = 16.5 and 35.2 THz, found in Fig. 2(d). In the beat-frequency–resolved 2D spectra, we find many peaks hidden by a strong stationary signal ($E_{beat} \approx 0$ THz).

The progression of the peaks along the excitation frequency axis can be observed clearly in the 2D map at E_{beat} = 16.5 THz. All peaks belonging to the progression are broad along the detection frequency axis. The progression of the peaks along the excitation frequency axis, observed in the beat-frequency–resolved 2D-ES is not visible in the absorption spectrum, owing to the occurrence of inhomogeneous broadening. Progression A starts at E_{exc} = 510 THz with an interval of 35 THz on the excitation frequency axis. The frequency of 510 THz is close to the peak frequency in the absorption spectrum, indicating that the pump pulse excites the molecules to the bottom of the first electronically excited state.

At E_{beat} = 35.2 THz, peak B1 is found at the diagonal position of the 2D map. Both the excitation and detection frequencies at this diagonal position are approximately 512 THz, which is the peak frequency of the absorption spectrum shown in Fig. 2(a). The other diagonal peak, B2, is also found at approximately E_{exc} = E_{det} ≈ 550 THz, which is close to the shoulder in the absorption spectrum. Weak cross-peaks B3 and B4 are observed at off-diagonal positions (E_{exc}, E_{det}) = (512 THz, 550 THz) and (550 THz, 512 THz), respectively.

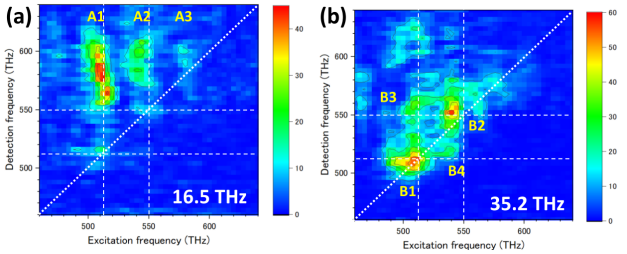

Fig. 3. Beat-frequency–resolved 2D spectra of RasM. The 2D spectra (a) and (b) are extracted from the total 2D spectra at the beat frequencies of E_{beat} = 16.5 and 35.2 ± 1 THz, respectively.

We will extend this method to observe the quantum coherence between the exciton states in a RasM dimer or heterodimer of RasM and its derivative. Because we have already assigned vibrational coherence to the RasM monomer, we can easily distinguish it from the coherence between the exciton states. This method can be applied to natural and artificial photosynthesis proteins to investigate the relationship between the coherence phenomena and high-efficiency unidirectional energy transfer during photosynthesis.

Acknowledgements

The authors thank Y. Yonetani and A. Tanaka at QST for the valuable discussions on quantum coherence within biomolecules. We also thank A. Ishizaki at the Institute for Molecular Science for the valuable comments on 2D-ES.

References

1. J. Cao et al., Sci. Adv. **6** eaaz4888. (2020).
2. G. D. Scholes et al., Nat. Chem. **3** 763-774. (2011).
3. A. Ishizaki, G. R. Fleming, Annu. Rev. Condens. Matter Phys. **3** 333-361. (2012).
4. F. D. Fuller et al., Nat. Chem. **6** 706-711. (2014).
5. E. Romero et al., Nat. Phys. **10** 676-682. (2014).
6. M. Tsubouchi et al., arXiv:2211.02220. (2022).
7. C.-H. Lu et al., Optica **1** 400-406. (2014).
8. C. P. Hauri et al., Appl. Phys. B **79** 673-677. (2004).
9. D. B. Strasfeld, S.-H. Shim, M. T. Zanni, in *Advances in Chemical Physics*, pp. 1-28 (2009).